Available online at www.sciencedirect.com
ScienceDirect
Journal of Power Sources 174 (2007) 856–860
JOURNAL OF POWER SOURCES
www.elsevier.com/locate/jpowsour

Short communication

Development of a universal modeling tool for rechargeable lithium batteries

Matthieu Dubarry, Bor Yann Liaw *

Hawaii Natural Energy Institute, School of Ocean and Earth Science and Technology, University of Hawaii at Manoa, 1680 East West Road, POST 109, Honolulu, HI 96822, USA

Available online 28 June 2007

Abstract

An interesting universal modeling tool for rechargeable lithium batteries is presented in this paper. The generic model is based on an equivalent circuit technique commonly used in electrochemical impedance characterization. Therefore, the parameters used in the model can be easily parameterized from the electrochemical impedance derivations, which provide a convenient integration with experimental cell characterizations. Such integration offers the universality in this modeling approach.

Keywords: Universal model; Rechargeable lithium batteries; Equivalent circuit; Impedance; Life prediction; Computer simulation

1. Introduction

Rechargeable lithium batteries (RLB) remain to be the battery of choice for consumer electronics, telecommunication, space, hybrid power sources, and military applications due to their availability, maturity, and cost. For reliable operation of RLB in these applications, accurate life prediction capability is thus of significant value to the industry and consumers. Predicting battery performance and service life is a very challenging task, but reward for such a capability is very attractive. The ability to predict battery life accurately can enhance the convenience, reliability, utility, and mobility of RLB as power sources in real-life applications. However, predicting battery service life in practical applications remains problematic, due to the lack of established techniques to achieve such prediction, even with drastic improvements in computer power and software capability [1–8] since 1990s. Meanwhile, experimental techniques that allow detailed investigation of interfacial and bulk properties of electrode materials have contributed to a better understanding of cell performance and degradation [9]. It is considerably easier now to develop an integrated battery testing and simulation capability to assist battery R&D and operation [10].

A viable approach to enable battery performance and service life prediction is to develop realistic computer simulation capabilities. A practical simulation and modeling tool, however, needs to bridge the gap between laboratory test results and real-life data so that laboratory test results can be used to predict anticipated performance in real life.

In this work, we present an effort to use an equivalent circuit model (ECM) to develop a battery simulation tool for lithium ion cells. This generic modeling approach is simple but useful since it can allow accurate prediction of battery performance using data collected in the laboratory tests [8]. Since the modeling approach uses parameters derived from typical electrochemical characterizations, such as charge and discharge curves, this modeling tool can be very versatile to simulate any cell chemistry with minimal details in the chemistry itself. Therefore, this approach is more phenomenological than mechanistic.

2. Principles

The simplicity of an ECM approach relies on its direct correspondence with complex impedance characteristics of the cell; therefore, this approach can simulate battery performance characteristics directly from monitoring and measuring conditions of the cell operation. Conventionally, we use equivalent circuits to interpret the data obtained from electrochemical impedance spectroscopic (EIS) measurements. Inversely, in the ECM approach, the associated equivalent circuit can be used as the tool to predict battery behavior. Fig. 1 presents an example of an ECM used in this study, where V_o corresponds to the open cir-

* Corresponding author. Tel.: +1 808 956 2339; fax: +1 808 956 2336.
E-mail address: bliaw@hawaii.edu (B.Y. Liaw).

0378-7753/$ – see front matter © 2007 Elsevier B.V. All rights reserved.
doi:10.1016/j.jpowsour.2007.06.157

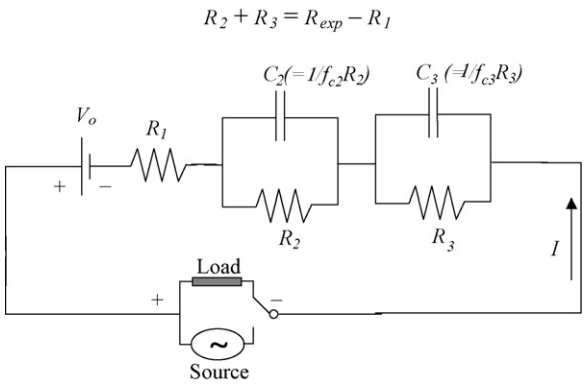

Fig. 1. Schematic representation of an equivalent circuit model (ECM) used in the work.

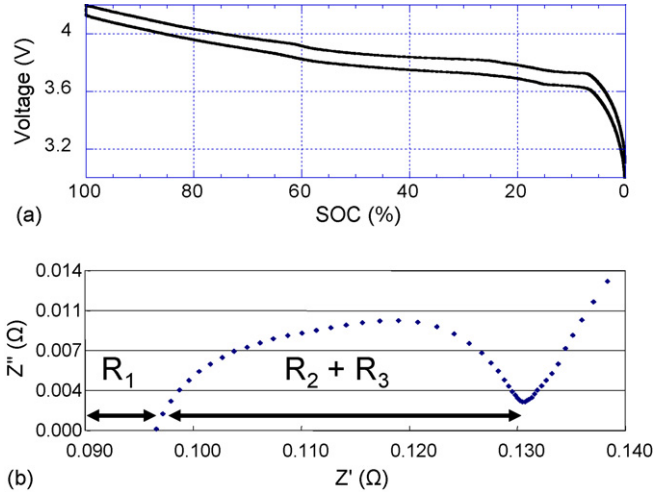

Fig. 2. (a) C/25 charge and discharge curves as a function of SOC and (b) Nyquist plot from a complex impedance measurement at 100% SOC.

cuit voltage (OCV) of the cell as a function of the state-of-charge (SOC); R_1 is the ohmic contribution including contact resistance, which is usually constant and can be determined using the EIS technique. It is also logical to determine R_2 and R_3 using the EIS technique. Nonetheless, in practical applications, this process is time consuming and often subject to human intervention, as they are, most of the time, SOC-dependent.

A simplified approach can be used to derive R_2 and R_3 from the Ohmic law, i.e., $V = IR$. This simple relation can be used to determine the experimental resistance (R_{exp}) as a function of the SOC. More precisely, from the experimental data we can derive R_{exp} using $\Delta V = R_{exp}\ \Delta I$ in the charge discharge cycles and with a close approximation of *IR*-free voltage to estimate OCV. As long as we can determine a polarization potential difference between two rates, we can estimate R_{exp}. Knowing R_{exp}, we can further estimate the *IR*-free voltage, which can be used to further infer the SOC for the specific R_{exp}; therefore,

$$\Delta V \Rightarrow V_{OCV} - V_{C/n} = R_{exp}(I_{OCV} - I_{C/n}) \Leftarrow R_{exp}\Delta I$$

whereas, $I_{OCV} = 0$,

$$R_{exp} = -\frac{(V_{OCV} - V_{C/n})}{I_{C/n}}$$

and,

$$R_2 + R_3 = R_{exp} - R_1$$

The difficulty of this approach is to determine the SOC of the cell precisely. This issue has been discussed elsewhere [11,12]. The model described in [8], which is similar to the present work but using a different ECM to describe the cell characteristics, did not employ SOC based on thermodynamic consideration. Instead, it used the SOC determined by capacity-based interpretation according to [13] in the simulation. In addition, the prior model did not consider R_1 and R_2 as rate-dependent parameters. Such a rate-dependent consideration was employed in the current model, as represented in R_3. This consideration does improve the accuracy of the prediction.

3. Experimental

A commercial graphite (G) | $LiCoO_2$ cell was used in this work as a model system for study. The cell has been cycled at C/25, C/5 and C/3 using a Solartron 1470 station. The cycling data of the cell under C/25 charge and discharge regimes were used as the benchmark of the cell, so a definitive capacity versus SOC relationship can be established (Fig. 2a) for this particular chemistry. The cycling data obtained under C/5 and C/3 rate were used to determine the rate dependence of the parameters in the model. The parameters obtained in this procedure allow the simulation of cell performance.

As shown in [11,12], the cause of capacity loss in the cell is often due to rate-associated undercharge. In order to determine the degradation of the cell, a second cell was subjected to a cycle life evaluation using the dynamic stress test (DST) schedule and reference performance tests (RPT), according to the U.S. Advanced Battery Consortium (USABC) test procedures [13]. The RPT consists of four core tests; three on the cell capacity under constant current, constant power, and DST regimes; and one related to the test of SOC-dependent peak power capability. The charge regime was performed with the algorithm provided by the manufacturer, which is a two-step constant-current constant-voltage (CC–CV) procedure.

4. Results and discussion

The C/25 cycling behavior is considered close to OCV (Fig. 2a) and R_1 was determined by EIS (Fig. 2b). In the first set of experiments, we considered R_2 and R_3 SOC-dependent. We, however, did not separate R_2 and R_3. Instead, a lumped R will be used to represent $R_2 + R_3$. In order to verify if R is rate dependent, we calculated the resistance values from C/5 and C/3 discharge and charge regimes, respectively.

Fig. 3a presents the results of C/5 cycle (symbols) and the curve obtained from linear interpolation of experimental data (solid line). Due to undercharging, no experimental data were available in the charge regime between 84% and 100% SOC.

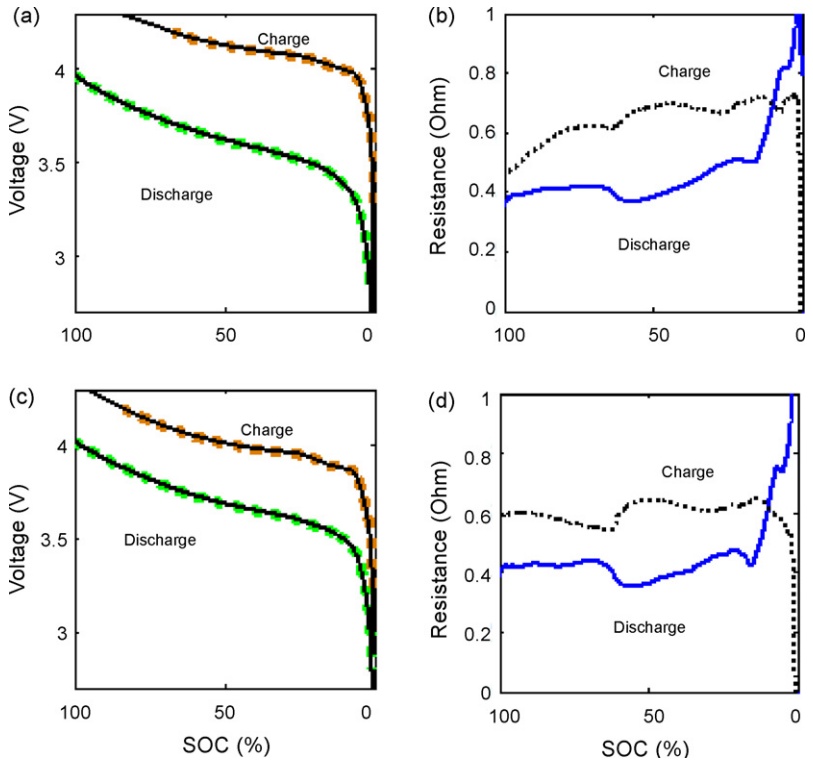

Fig. 3. (a) Experimental (dotted line) and interpolated (solid line) C/5 cycle. (b) Calculated $R_{C/5\_dis}$ (solid line) and $R_{C/5\_ch}$ values (dotted line). (c) Experimental (dotted line) and interpolated (solid line) C/3 cycle. (d) Calculated $R_{C/3\_dis}$ (solid line) and $R_{C/3\_ch}$ values (dotted line).

Through extrapolation, we projected a hypothetic charge curve in this SOC range from the last three charging data points that provide the trend line. The extrapolation allowed us estimate approximated resistance values for this SOC range. Fig. 3b shows the calculated discharge (solid line) and charge (dotted line) resistance values. They are denoted as $R_{C/5\_dis}$ and $R_{C/5\_ch}$ for the discharge and charge regime, respectively. Using the same method, we obtained Fig. 3c and d for C/3 cycle.

By comparing Fig. 3b and d, as shown in Fig. 4a and b for discharge and charge regimes, respectively, we noticed that there are some distinct differences between the C/5 and C/3 resistance values and trends. In the discharge regime, the shape of the resistance curves is very similar, while the difference between the two varies slightly, depending on SOC. In the charge regime, both the shape and disparity between the two resistance curves become more noticeable, particularly in the regions above 65% SOC and below 15% SOC. It should be noted that the difference in the charge resistance at high SOC (i.e., >65%) might be originated from the extrapolation, as the charge potential for SOC > 65% at C/3 was estimated without validation. The observation of resistance disparity warranted us to conduct the following analysis to assess the sensitivity of these differences in model prediction with rate dependency.

With $R_{C/3\_dis}$ and $R_{C/3\_ch}$ values, a synthetic C/5 cycle has been simulated from the model and the charge and discharge curves are presented in Fig. 5a. In comparison with the experimental data (dotted lines), the simulated curves (solid lines) are fairly close to the experimental results. Upon close exam-

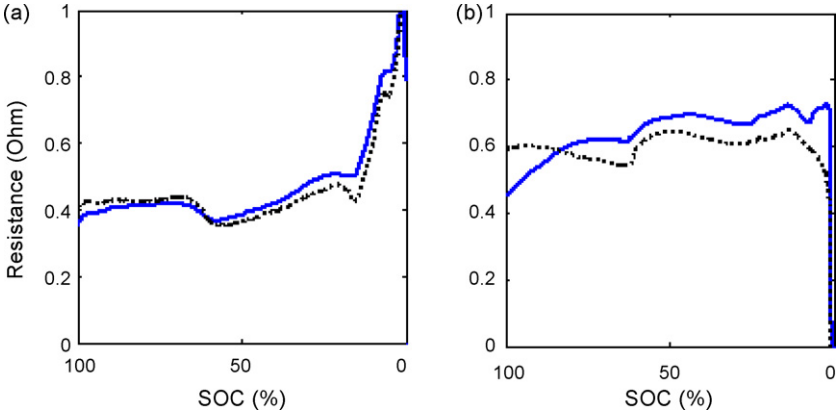

Fig. 4. Comparison of (a) $R_{C/5\_dis}$ and $R_{C/3\_dis}$, and (b) $R_{C/5\_ch}$ and $R_{C/3\_ch}$ ($R_{C/5}$: solid lines, $R_{C/3}$: dotted lines).

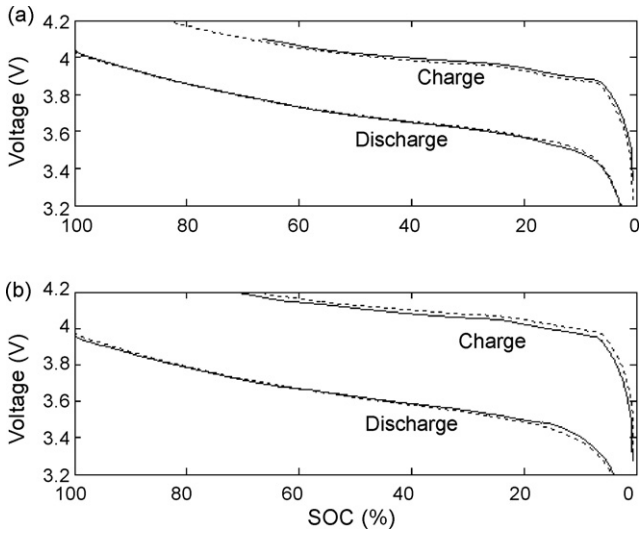

Fig. 5. (a) Simulated C/5 cycle using SOC-dependent $R_{C/3}$ values. (b) Simulated C/3 cycle using SOC-dependent $R_{C/5}$ values. (Solid lines: simulated; dotted lines: experimental).

ination, we found that the C/5 polarization potential using the C/3 resistance seemed overestimated, since the simulated discharge curve is under the experimental data; and, vice versa, we observed that the simulation is over the experimental data in the charge curve.

If we employed $R_{C/5\_dis}$ and $R_{C/5\_ch}$ to derive C/3 cycle, as shown in Fig. 5b, the simulated discharge and charge curves were then displaced by underestimations in polarization potential, as exhibited by the discernable disparity between the simulated curves and the experimental results in Fig. 5b.

In light of these results, we suspect that the resistance is rate dependent. We also noticed that the shape of the resistance curve at different rates exhibits abrupt changes that is not monotonic but in a complex fashion. It is therefore plausible that the variation of the resistance curves with SOC may be related to phase transformations, including staging of the anode material. Interestingly, the regions where the resistance curve showed the abrupt change in trend are in agreement with the region where the staging was expected to occur. This observation is comprehensible. Since staging exhibits a potential change within a narrow composition range, we shall expect an abrupt change in the cell voltage reflecting the staging phenomenon. Therefore, an abrupt change in resistance curve should be expected.

To address the rate dependent issue, we use the following approach to assess the sensitivity of the rate dependence. If the rate dependence of the resistance was weak, we applied $R_{C/5}$ and $R_{C/3}$ to simulate C/2 and 1C discharge curves (Fig. 6). The results of both C/2 and 1C simulations show that the portion of the curves in the high SOC (>65%) region is in agreement with experiments. Nevertheless, as soon as the anodic staging occurs, the simulation began to show significant disparity with the experimental data. The degree of mismatch increases with the difference in rate. An even higher disparity is observed when the last staging occurs.

It becomes apparent now that the phase transformation, such as the staging of the anode, plays a unique role in the

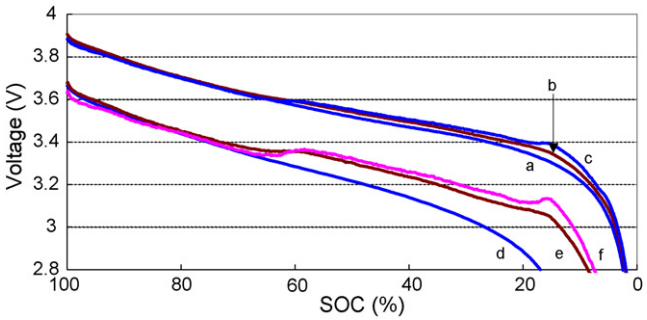

Fig. 6. Discharge curves at C/2 and 1C rate. Curves (a) and (d) are experimental data. Curves (b) and (e) are calculated from $R_{C/3}$. Curves (c) and (f) are from $R_{C/5}$.

resistance correspondence with rate in charge and discharge regimes. This correspondence of resistance with rate and SOC is depicted in Fig. 7a. Comparing the difference in resistance curves between C/5 and 1C, as shown in Fig. 7b, we begin to observe the rate effect. One can perceive that, when the rate is low, the phase transformation remains distinct with the time frame of the reaction kinetics. The abrupt change in the electrochemical potential within the phase boundaries is therefore quite visible. As rate increases, the distinct feature in phase transformation is becoming indiscernible, as reflected in the cor-

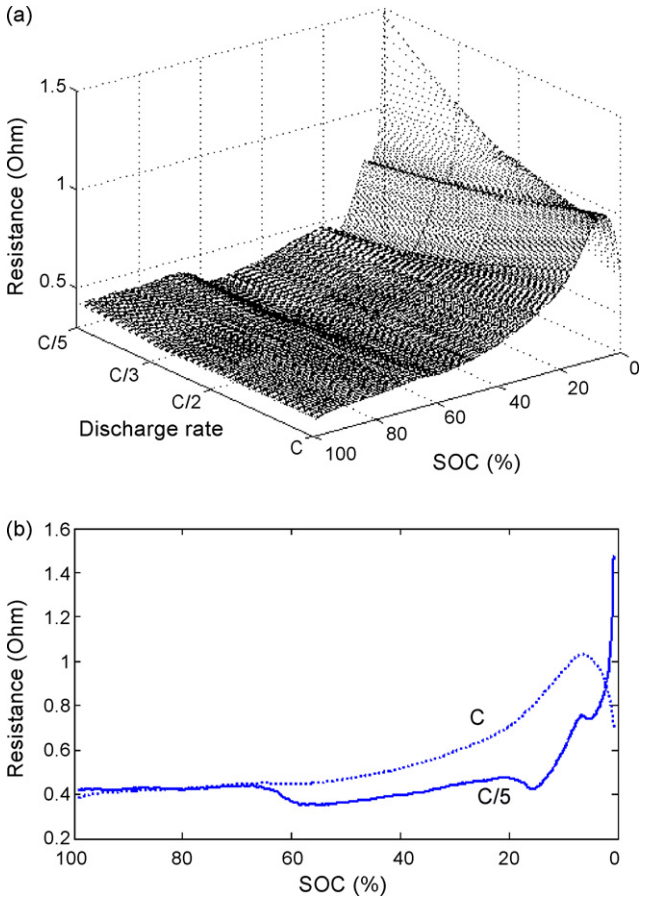

Fig. 7. (a) Correspondence of cell resistance as a function of SOC and discharge rate, and (b) comparison of C/5 and 1C resistance curves.

responding resistance curve. Eventually, the resistance curve at 1C becomes smooth and featureless with SOC. A high fidelity of simulation requires us to pay attention to these details. It is also useful to point out that those details can be derived from experimental data, with less degree of emphasis on mechanistic understanding.

5. Conclusion

A simple, general purpose, cost-effective battery modeling approach using equivalent circuit model can offer high fidelity simulation of battery performance. When we paid attention to rate and SOC dependence of resistance, the simulation leads to an improved prediction of cell performance. This simulation tool can be integrated with cell testing to derive useful information for improving battery design and performance. This integrated testing and simulation (ITS) approach may allow us to develop a sophisticated battery model without detailed mechanistic understanding of the chemistry.

Acknowledgements

This work is performed under a contract (HEVDP Contract # 46049, Supplement 5) with the Hawaii Center for Advanced Transportation Technologies (HCATT) under the support (Federal Other Transaction Agreement No. DTRS56-99-T-0017) from the U.S. Air Force Advanced Power Technology Office (APTO) at the Robins Air Force Base in Georgia.

References

[1] J. Newman, K.E. Thomas-Alyea, Electrochemical Systems, third ed., Electrochemical Society Series, Wiley-Interscience, John Wiley & Sons, Inc., Hoboken, NJ, 2004.
[2] E. Barsoukov, J.H. Kim, C.O. Yoon, H. Lee, Solid State Ionics 116 (1999) 249.
[3] C. Fellner, J. Newman, J. Power Sources 85 (2000) 229.
[4] B. Wu, M. Mohammed, D. Brigham, R. Elder, R.E. White, J. Power Sources 101 (2001) 149.
[5] G.L. Plett, J. Power Sources 161 (2006) 1369.
[6] R. Spotnitz, J. Power Sources 113 (2003) 72.
[7] P. Ramadass, B. Haran, P.M. Gomadam, R.E. White, B.N. Popov, J. Electrochem. Soc. 151 (2004) A196.
[8] B.Y. Liaw, R.G. Jungst, G. Nagasubramanian, H.L. Case, D.H. Doughty, J. Power Sources 140 (2005) 157.
[9] FY2006 Progress Report for Energy Storage Research and Development, U.S. Department of Energy, Office of FreedomCAR and Vehicle Technologies, Washington, D.C., 2006.
[10] B.Y. Liaw, X.G. Yang, K.P. Bethune, Solid State Ionics 152–153 (2002) 51.
[11] M. Dubarry, V. Svoboda, R. Hwu, B.Y. Liaw, Electrochem. Solid State Lett. 9 (2006) A454.
[12] M. Dubarry, V. Svoboda, R. Hwu, B.Y. Liaw, J. Power Sources 174 (2007) 1121.
[13] Electric Vehicle Battery Test Procedures Manual, Revision 2, USABC/US DOE/INEL, January 1996.